Cd_2SnO_4 AS FRONT CONTACT FOR CdS/CdTe SOLAR CELLS

K. Oehlstrom [1], V. Sittinger [2], S.J.K. Friedmann [3], A.E. Abken [1], R. Reineke-Koch [1], J. Parisi [4]
[1] Institut für Solarenergieforschung GmbH (ISFH), Außenstelle Hannover, Sokelantstraße 5, D-30165 Hannover, Germany,
phone: +49(0)511 35850-174, fax: +49(0)511 35850-110, email: k.oehlstrom@isfh.de
[2] Fraunhofer Institut für Schicht- und Oberflächentechnik (IST), Bienroder Weg 54 E, 38108 Braunschweig, Germany,
phone: +49(0)531 2155-512 fax: +49(0)531 2155-900, email: sittinger@ist.fhg.de
[3] Niedersächsisches Landesmuseum Hannover, Willy-Brandt-Allee 5, 30169 Hannover, Germany,
phone: +49(0)511 9807-654
[4] Universität Oldenburg, Carl-von-Ossietzky-Str. 9-11, 26111Oldenburg, Germany,
phone: +49(0)441/798-3402, fax: +49(0)441 798-3326, email: juergen.parisi@ehf.uni-oldenburg.de

ABSTRACT

Cd_2SnO_4 (CTO) transparent conducting oxide (TCO) is chosen to replace the In_2O_3:Sn/SnO_2 layers in CdS/CdTe thin film solar cells. Lower material costs and one layer less than the conventional ITO/SnO_2 front contact means a significant cost reduction in solar cell production. Furthermore Wu et al.[1] demonstrated superior optical, electrical and morphological properties of the CTO films compared to other TCO`s. In addition Indium is supposed to diffuse from incomplete oxidised ITO-layers into the CdS/CdTe-layers. Indium acts as donator in CdTe and compensates its desired p-type character. The CTO-layers are prepared by reactive rf-magnetron sputtering from a Cd/Sn-alloy target with a Cd:Sn composition of 2:1. The morphology of the CTO-layers is investigated by atomic force microscopy (AFM) and scanning electron microscopy (SEM). The optical and electrical properties are characterised with transmission/reflection measurements, ellipsometry, Hall-effect- and conductivity measurements, respectively. A CdS/CdTe solar cell with Cd_2SnO_4 as TCO with conversion efficiency of 7.5% has been prepared and is characterised with current-voltage and quantum efficiency measurements.
Keywords: TCO Transparent Conducting Oxides - 1: Optical Properties - 2: CdTe – 3

1. INTRODUCTION

The front contact in solar cells determines the amount of light introduced into the absorbing layers as well as the transport of the generated charge carriers. A good transmittance with simultaneous high conductivity is therefore desirable. ITO layers show good performance in both properties but introduce some problems in CdS/CdTe-solar cell preparation. Indium is supposed to diffuse from incomplete oxidised ITO-layers into the CdS/CdTe-layers. Indium acts as donator in CdTe and compensates its desired p-type character. Another important aspect is the rather high cost for Indium. Alternatively, fluorine doped SnO_2 and aluminium doped ZnO have been investigated by Romeo et al. [2]. Both TCO`s resulted in poor performance of the CdS/CdTe solar cells compared to ITO front contacts. In 1997 Wu et al. [1] reported a CdS/CdTe solar cell with conversion efficiency of 13.7% with Cd_2SnO_4 (CTO) as TCO. Further developments leaded to a new world-record efficiency at NREL of 16.4% [3]. Further advantages of CTO are its easy paternability and mechanical stability.

In this work the morphology, the optical and the electrical properties of CTO-films have been investigated. The films have been prepared by reactive rf-magnetron sputtering in oxygen atmosphere from a Cd/Sn-alloy target with Cd:Sn composition of 2:1. The preparation conditions have been as follows:

- Base pressure: $p_B = 4*10^{-6}$ mbar
- Substrate temperature: $T_S = 625$ K
- Oxygen partial pressure: $p_{O2} = 5*10^{-3}$ mbar
- Sputtering power: P = 1.6 Wcm^{-2}

2. MORPHOLOGY

The morphology of the CTO has been investigated by atomic force microscopy (AFM) and scanning electron microscopy (SEM). Figure 1 shows the AFM image of a CTO layer of 270 nm thickness and a resistivity of $3.5*10^{-4}$ Ωcm.

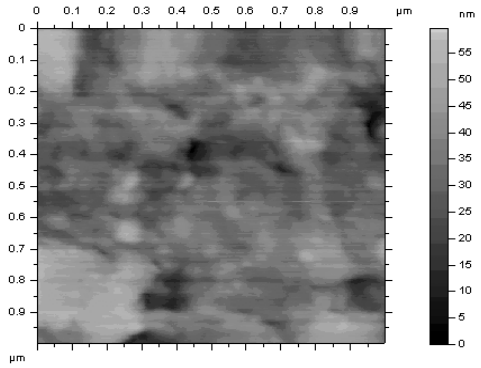

Figure 1: AFM image of the Cd_2SnO_4 surface. An area of 1 × 1 μm^2 has been scanned. A RMS-roughness of 8.5 nm has been calculated.

The image exhibits lateral structures with width between 50–80 nm as well as larger structures of some 100 nm in diameter. The Cd_2SnO_4 film exhibits a rough surface with a calculated RMS-roughness of 8.5 nm. The height profile of this image exhibits lateral structures of the smaller type (Figure 2). Figure 2 also shows a 1 µm sector from a height profile taken from a SEM image of the same sample. It shows lateral structures with dimensions of 100-200 nm.

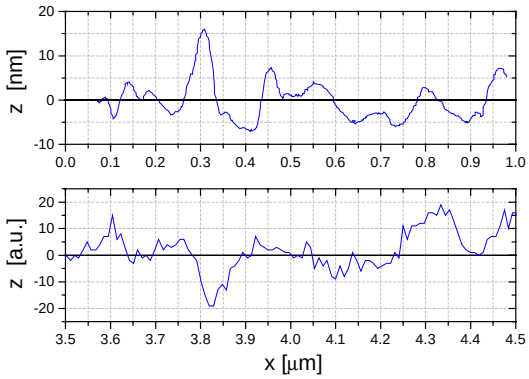

Figure 2: Cross-section from AFM- (top picture) and SEM-images (bottom picture). The AFM-profile exhibits a maximum height difference of 25 nm.

3. OPTICAL PROPERTIES

The optical properties of the Cd_2SnO_4 layers have been investigated by transmission/reflection and ellipsometrical measurements. To determine the refractive index n(λ) and the extinction coefficient k(λ), two different modified Lorentz-Drude models have been used. In the Lorentz-Drude model the dielectric function ε(ω) is given by:

$$\varepsilon(\omega) = \varepsilon_\infty + \sum_k \frac{\omega_{pk}^2}{\omega_{0k}^2 - \omega^2 - i\,\gamma_k\,\omega}$$

The index k counts the oscillator modes, i is the imaginary unit, ε_∞ is the dielectric constant in the high frequency region, ω_{pk} and ω_{0k} are the plasma and the resonance frequency of the k^{th} mode, respectively. In the Drude model, where $\omega_{0k} = 0$, the phenomenological attenuation constant γ_k is inverse proportional to the relaxation time τ of the electrons. The classical Lorentz oscillator as given in the formula above considers the absorption at the resonance frequency as Lorentz-peak shaped, which describes only the natural line-width. More realistic modifications of this model result in Gauß shaped, as in [4], or asymmetrically broadened Lorentz peaks with prefactors proportional to ω^2 as in [5]:

Gauß-broadened Lorentz-Drude model for one oscillator as proposed by Brendel and Bormann [4].
Here, σ denotes the standard deviation of the Gauß curve:

$$\varepsilon(\omega) = \varepsilon_\infty + \frac{1}{\sqrt{2\pi}\sigma}\int_{-\infty}^{+\infty} dx \exp\left(-\frac{(x-\omega_p)^2}{2\sigma^2}\right)\frac{\omega_p^2}{\omega_0^2 - \omega^2 - i\gamma\omega}$$

Lorentz-Drude model for one oscillator as proposed by Leng et al. [5]:

$$\varepsilon(\omega) = \varepsilon_\infty + \frac{C_0}{\omega^2}\{\, e^{i\beta}(\omega_0 - \omega - i\gamma)^\mu + e^{-i\beta}(\omega_0 + \omega + i\gamma)^\mu$$
$$- 2\,\mathrm{Re}\left[e^{-i\beta}(\omega_0 + i\gamma)^\mu\right] - 2i\mu\omega\,\mathrm{Im}\left[e^{-i\beta}(\omega_0 + i\gamma)^{\mu-1}\right]\}$$

Equal symbols have the same meaning in both formulas. The ellipsometrical data together with the T/R-spectra have been simulated with both models. The results are depicted in Figures 3 and 4. Both models have been used with a single oscillator and a Drude term, where the resonance frequency ω_0 is set to zero. While the Lorentz-oscillator describes the fundamental absorption-edge, the Drude term describes the influence of free electron absorption.

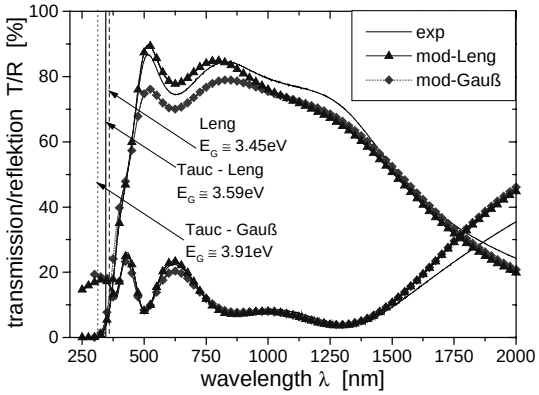

Figure 3: Reflection/Transmission spectra of Cd_2SnO_4. Measured data (line), model Gauß (diamond), model Leng (up triangle). Determined band gap energies are depicted.

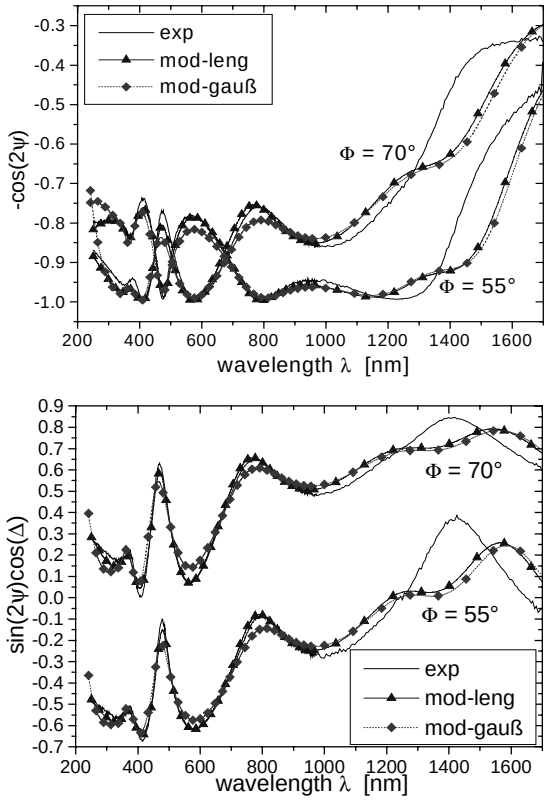

Figure 4: The re-scaled ellipsometric parameters ψ (top picture) and Δ (bottom picture).
The symbols for experimental and simulated data are the same as in Figure 3.

As can be seen from the spectra in Figure 3 and 4, the Leng model fits better to the data in the short wavelength

range near the absorption edge. The deviation of the simulation from the experimental data in the infrared region demonstrates the misfit of the free carrier model to the transport processes in the material. Further work has to be done in this field, to obtain correct fitting curves.
Nevertheless, conductivity and thickness obtained from the simulation are in good agreement with values obtained from more directly methods (compare Table I).
The calculated functions n(λ) and k(λ) are plotted in Figure 5. One can see clear deviations resulting from the two different models mainly at the vicinity of the absorption edge and in the infrared region.

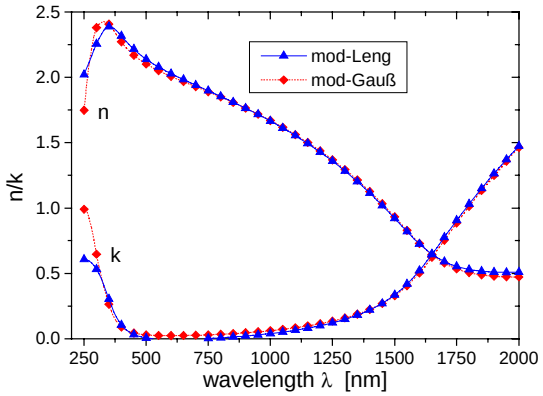

Figure 5: Refractive index and extinction coefficient calculated with the two models from Brendel et al. [4] (diamond) and Leng et al. [5] (up triangle).

To simulate the data in the infrared region, the Drude model for free electrons has been used. Within this model the conductivity σ is given by:

$$\sigma = \omega_p^2 \varepsilon_0 \tau$$

ε_0 denotes the electric field-constant.
The plasma frequency ω_p and the relaxation time $\tau = 1/\gamma$ are fit parameters. The resulting values for τ, σ and film thickness D are given in Table I together with some directly measured values.

Table I: Film thickness, conductivity σ, bandgap E_{gap} and relaxation time τ as received by different methods.

Method	D nm	σ $[\Omega^{-1}cm^{-1}]$	E_{gap} [eV]	τ $[10^{-15}s]$
Gauß	240	$2.5*10^3$	3.9 (Tauc)	4.95
Leng	237	$2.2*10^3$	3.6 (Tauc) 3.45 (sym)	4.28
α-step	225	-	-	-
vdPauw	-	$2.8*10^3$	-	-

The bandgap energies given in Table I have been received directly from the simulation (Leng model) or from $(\alpha h\nu)^2$ vs. hν plots (marked as "Tauc" in the table), assuming a direct bandgap. The absorption coefficient α is given by: $\alpha = 4\pi k/\lambda$.

4. ELECTRICAL PROPERTIES

The conductivity σ, electron mobility μ_H, free electron concentration n_e, effective mass m^*_e and the mean free path Λ_e of the electrons have been determined by van der Pauw and Hall-effect measurements. The free electron concentration and the electron mobility are given by:

$$n_e = -\frac{1}{eR_H} \qquad \mu_H = \frac{\sigma}{en_e} = \sigma\left|R_H\right|$$

In this formulas e denotes the electron charge.
While Hall-coefficient R_H and therefore the free electron concentration are found to be independent of temperature, conductivity and electron mobility exhibit a weak temperature dependence, as shown in Figure 6. The temperature dependence of the conductivity shows the characteristic behaviour of metallic conduction: A linear dependence for high temperatures resulting from phonon scattering. A constant value is reached below a certain temperature, which results from defects within the material. From the temperature independence of the free electron concentration and the characteristic course of the conductivity the degeneracy of the material is concluded and the utilisation of the Drude model for the free electron gas is therefore justified.

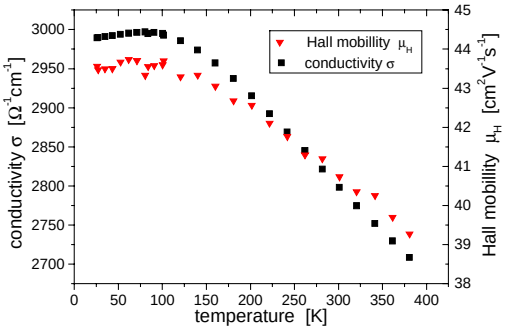

Figure 6: Conductivity σ (square) and Hall mobility μ_H (down triangle) vs. temperature.

The free electron concentration has been determined to:

$$n_e = 4.3\times10^{20}\ cm^{-3}$$

Within the Drude model for free electrons the conductivity is related to the free electron concentration and the effective mass via:

$$\sigma = \frac{n_e e^2 \tau}{m_e^*} = \omega_p^2 \varepsilon_0 \tau \quad \Rightarrow \quad m_e^* = \frac{n_e e^2}{\varepsilon_0 \omega_p^2}$$

Here, τ and ω_p denote the relaxation time and the plasma frequency determined by the optical simulations described in chapter 3. From this relation the effective mass follows to :

$$m_e^* = 0.24\, m_e$$

Where m_e represents the electron mass.
The mean free path between two collisions Λ_ε is given by:

$$\Lambda_e\left(\left|\mathbf{k}_F\right|\right) = v\left(\left|\mathbf{k}_F\right|\right)\tau\left(\left|\mathbf{k}_F\right|\right)$$

In the model of the conduction of metals $v(\mathbf{k}_F)$ is the velocity of the contributing electrons at the Fermi level, with a wave vector $\mathbf{k}_F$. It is obtained via an easy approximation for the radius of the Fermi-globe:

$$v\left(\left|\mathbf{k}_F\right|\right)=\frac{\hbar\left|\mathbf{k}_F\right|}{m_e^*} \quad with \quad \left|\mathbf{k}_F\right|=\sqrt[3]{3\pi^2 n_e}$$

Using the relaxation times τ given from the optical simulations (Table I), the carrier concentration and the effective mass as given above, one obtains:

$$\Lambda_{e,Leng} = 4.8\,nm$$

$$\Lambda_{e,Gauß} = 5.6\,nm$$

Considering the deviations of the Drude model in the simulations of the optical data, those values have to be regarded with care. Still the obtained values are in realistic regions. Consideration of scattering mechanisms in electron transport models should yield more accurate results.

5. THE Cd_2SnO_4/CdS/CdTe/Ni SOLAR CELL

A CTO film of 225 nm thickness and a sheet resistance of R_{sq}=16.56 Ω has been used as front contact for a CdS/CdTe solar cell. The cell was prepared in superstrate configuration in the following order:

float glass/CTO/CdS/CdTe/Ni.

After CdTe deposition an activation step and etching of the cell with a mixture of phosphoric and nitric acid followed.

Figure 7 shows the external and the internal quantum efficiency EQE/IQE of the cell. The IQE reaches a plateau between 520 nm and 830 nm of nearly 90%. The inset shows dark and illuminated current-voltage curves.

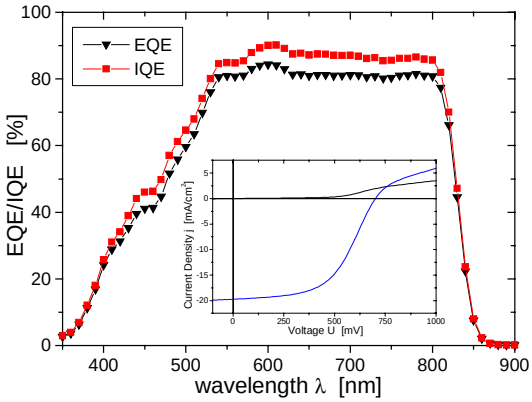

Figure 7: External (down triangle) and internal quantum efficiency (square) of the CdS/CdTe solar cell with CTO as front contact.
Inset: dark and illuminated current-voltage curves.

The characteristic parameters of the cell are as follows: Conversion efficiency η = 7.5%, fill factor FF = 54.1%, open circuit voltage U_{oc} = 701 mV, short current density j_{sc} = 19.7 mA/cm^2.

6. CONCLUSIONS

Transparent conducting Cd_2SnO_4 layers have been prepared. The morphology as well as the optical and electrical properties have been characterised.
The refractive index n(λ) and the extinction coefficient k(λ) have bee determined by modelling the dielectric function using Gauß and Leng broadened Lorentz oscillators. It is shown, that the model from Leng et al. fits better for wavelength near the bandgap. In the infrared region the Drude model was applied. This model exhibits rather large deviations. Further work has to be done in this field.
Using Hall-effect and conductivity measurements the temperature dependent mobility and the carrier concentration have been determined. Using the Drude model for free electrons, effective mass m^*_e and the mean free path Λ_e of the electrons have been calculated.
A CdS/CdTe solar cell with CTO as front contact has been prepared. A conversion efficiency of 7.5% was achieved in the first attempt.

ACKNOWLEDGEMENTS

We acknowledge the Bundesministerium für Wirtschaft und Technologie for financial support (Contract No: 0329787). The authors also want to thank M. Munzel, C. Deibel and H. Koch from the University of Oldenburg for support and advice during the Hall measurements. We also thank H.-G. Holtorf from the University of Oldenburg for the support and help during the AFM measurements.

REFERENCES

[1] X. Wu, P. Sheldon, T.J. Coutts, D.H. Rose, W.P. Mulligan, H.R. Moutinho, NREL/SNL Photovoltaics Review (1997), AIP Press, New York

[2] A. Romeo, A.N. Tiwari, H. Zogg, M. Wagner, J.R. Guenter, Proceedings 2nd World Conference and Exhibition on Photovoltaic Solar Energy Conversion 6-10 July 1997 Vienna (Austria) 6-10

[3] X. Wu, T. Gessert, *http://www.nrel.gov/ncpv/hotline/04_01_cdte.html*

[4] R. Brendel, D. Bormann, J.Appl.Phys. 71(1), (1992) 1-6

[5] J. Leng, J. Opsal, H. Chu, M. Senko, D.E. Aspnes Thin Solid Films 313-314, (1998) 132-136